

ON THE FAINT-END OF THE GALAXY LUMINOSITY FUNCTION IN THE EPOCH OF REIONIZATION: UPDATED CONSTRAINTS FROM THE *HST* FRONTIER FIELDS

B. YUE,¹ M. CASTELLANO,² A. FERRARA,^{3,4} A. FONTANA,² E. MERLIN,² R. AMORÍN,^{5,6} A. GRAZIAN,² E. MÁRMOL-QUERALTO,⁷
M. J. MICHAŁOWSKI,⁸ A. MORTLOCK,⁷ D. PARIS,² S. PARSA,⁷ S. PILO,² P. SANTINI,² AND M. DI CRISCIENZO²

¹*National Astronomical Observatories, Chinese Academy of Sciences, 20A Datun Road, Chaoyang District, Beijing, 100012, China*

²*INAF - Osservatorio Astronomico di Roma, Via Frascati 33, I-00078 Monte Porzio Catone (RM), Italy*

³*Scuola Normale Superiore, Piazza dei Cavalieri 7, I-56126 Pisa, Italy*

⁴*Kavli IPMU (WPI), Todai Institutes for Advanced Study, the University of Tokyo, Japan*

⁵*Cavendish Laboratory, University of Cambridge, 19 JJ Thomson Avenue, Cambridge, CB3 0HE, UK*

⁶*Kavli Institute for Cosmology, University of Cambridge, Madingley Road, Cambridge CB3 0HA, UK*

⁷*SUPA, Scottish Universities Physics Alliance, Institute for Astronomy, University of Edinburgh, Royal Observatory, Edinburgh, EH9 3HJ, U.K.*

⁸*Astronomical Observatory Institute, Faculty of Physics, Adam Mickiewicz University, ul. Słoneczna 36, 60-286 Poznań, Poland*

ABSTRACT

Ultra-faint galaxies are hosted by small dark matter halos with shallow gravitational potential wells, hence their star formation activity is more sensitive to feedback effects. The shape of the faint-end of the high- z galaxy luminosity function (LF) contains important information on star formation and its interaction with the reionization process during the Epoch of Reionization (EoR). High- z galaxies with $M_{UV} \gtrsim -17$ have only recently become accessible thanks to the Frontier Fields (FFs) survey combining deep *HST* imaging and the gravitational lensing effect. In this paper we investigate the faint-end of the LF at redshift >5 using the data of FFs clusters Abell 2744 (A2744), MACSJ0416.1-2403 (M0416), MACSJ0717.5+3745 (M0717) and MACSJ1149.5+2223 (M1149). We analyze both an empirical and a physically-motivated LF model to obtain constraints on a possible turn-over of LF at faint magnitudes. In the empirical model the LF drops fast when the absolute UV magnitude M_{UV} is much larger than a turn-over absolute UV magnitude M_{UV}^T . We obtain $M_{UV}^T \gtrsim -14.3$ at 2σ confidence level (C.L.) for $z \sim 6$. In the physically-motivated analytical model, star formation in halos with circular velocity below v_c^* is fully quenched if these halos are located in ionized regions. Using updated lensing models and new additional FFs data, we re-analyze previous constraints on v_c^* and f_{esc} presented by Castellano et al. 2016a (C16a) using a smaller dataset. We obtain new constraints on $v_c^* \lesssim 57 \text{ km s}^{-1}$ and $f_{esc} \lesssim 63\%$ (both at 2σ C.L.) and conclude that there is no turn-over detected so far from the analyzed FFs data. Forthcoming JWST observations will be key to tight these constraints further.

Keywords: dark ages, reionization, first stars — galaxies: high-redshift — gravitational lensing: strong

1. INTRODUCTION

During the Epoch of Reionization (EoR, $6 \lesssim z \lesssim 30$), the intergalactic medium (IGM) was gradually ionized by energetic photons mainly emitted by the first galaxies. This in turn leads to the suppression of star formation in small galaxies, because their host halos hardly collect gas from ionized environment. This feedback effect raises the following questions: How faint the first galaxies could be and which halos could sustain star formation activity during the EoR?

According to the hierarchical structure formation scenario, smaller dark matter halos are much more common than bigger ones in the Universe, resulting in an overwhelming numerical abundance of very faint galaxies (Mason et al. 2015; Mashian et al. 2016; Finlator et al. 2017; Liu et al. 2016). Thereby, faint galaxies are promising candidates as main sources of reionizing photons (e.g. Bouwens et al. 2015a; Robertson et al. 2015; Castellano et al. 2016b), with a crucial contribution possibly coming from objects far below the detection limits of even the deepest existing surveys (Salvaterra et al. 2011; Robertson et al. 2013; Choudhury et al. 2008; Choudhury & Ferrara 2007; Dayal et al. 2013; Salvaterra et al. 2013). Moreover, faint galaxies are less clustered and their environment gas is less clumped, therefore they are more effective in reionizing the IGM.

To understand the role of star-forming galaxies in the reionization process, it is thus crucial to constrain their number density and star-formation efficiency by studying the UV luminosity function (LF) down to the faintest limits. The faint-end of the UV LF at high redshift has been found to have a steep slope at least down to absolute UV magnitudes $M_{UV} \sim -16$ (McLure et al. 2013; Bouwens et al. 2015b, B15 hereafter) in blank fields or even $M_{UV} \sim -12$ in gravitational lensing fields (Livermore et al. 2017, however see Bouwens et al. 2017b, these two are L17 and B17 hereafter). The high- z LFs have also been reconstructed from the number of ultra-faint dwarf galaxies – some of which are believed fossils of reionization galaxies – in the Local Group. For example, Weisz et al. (2014) conclude that the LF at $z \sim 5$ does not have any break at least down to $M_{UV} \sim -10$. At the same time, the detection of a break or turn-over would have an important implication related to the nature of the first galaxies and their contribution to reionization (e.g. Giallongo et al. 2015; Madau & Haardt 2015; Mitra et al. 2016).

Star formation in dark matter halos relies on the gas cooling process. However, both supernova explosion and ionizing radiation could prevent cooling. These feedback effects reduce the efficiency of star formation (Dayal et al. 2013; Xu et al. 2016; Sun & Furlanetto 2016) or even completely quench it, if the halo mass is too small. As a result, the number of galaxies hosted by small halos drops and we expect to see a “turn-over” in the faint-end of the galaxy LFs (Yue et al. 2016, Y16 hereafter). For example, in the “Cosmic Reion-

ization on Computers” (CROC) project, by galaxy formation and radiative transfer numerical simulations, it is found that the UV LF turns over at $M_{UV} \sim -14$ to ~ -12 (Gnedin 2016). And in the “FirstLight” project with radiative feedback effects, the LF has a flattening at $M_{UV} \gtrsim -14$ (with host halos’ circular velocity $\sim 30 - 40 \text{ km s}^{-1}$, Ceverino et al. 2017). Modifications of the initial power spectrum as in WDM cosmologies can also have a similar effect, see e.g. Dayal et al. (2015); Menci et al. (2016, 2017). Observations of galaxies around the turn-over would greatly increase our knowledge of the star formation physics in galaxies contributing most to reionization, and may directly answer our questions in the first paragraph (Yue et al. 2014).

Until now, there is no evidence that confirms or rules out the existence of such turn-over in both regular surveys and in gravitational lensing surveys, probably because their detection limits are still shallower than the turn-over absolute magnitude, see e.g. McLure et al. (2013); B15; Atek et al. (2015b); Atek et al. (2015a) (A15 hereafter); L17; Laporte et al. (2016); Ishigaki et al. (2017) (I17 hereafter).

With the help of strong magnification effects, the gravitational lensing provides an opportunity to detect galaxies below the detection limits of regular surveys. However, the cost is that the survey volume is reduced, and lensing models introduce extra uncertainties into the recovered intrinsic brightness of observed galaxies (B17).

The Frontier Fields (FFs) survey observed six massive galaxy clusters and their parallel fields in optical and near-infrared bands with the *Hubble*¹ and *Spitzer*² space telescopes (Lotz et al. 2017). These observations were also followed up by other observatories at longer and shorter wavelengths, e.g. *ALMA* (González-López et al. 2017a,b) and *Chandra* (Ogorean et al. 2015, 2016; van Weeren et al. 2017). Using the clusters as lenses, these images are deep enough to unveil faint galaxy populations at the EoR.

In Y16, we have derived the form of the LF faint-end during and after the EoR by assuming that the star formation in halos with circular velocity below a threshold v_c^* and located in ionized bubbles is quenched, where v_c^* is a free parameter. In Castellano et al. (2016a) (C16a hereafter) we constrained $v_c^* \lesssim 60 \text{ km s}^{-1}$ (2σ C.L.) by using the observed number counts of ultra-faint galaxies in two of the six FFs cluster fields, A2744 and M0416, and the *Planck*2015 results for τ (Planck Collaboration et al. 2016a).

Recently, by using two FFs clusters Abell 2744 (A2744) and MACSJ0416.1-2403 (M0416), L17 found that the faint-end of the LF at $z \sim 6$ always has steep slope ($\alpha \sim -2$) and

¹ <http://www.stsci.edu/hst/campaigns/frontier-fields/>

² <http://ssc.spitzer.caltech.edu/warmmission/scheduling/approvedprograms/ddt/frontier/>

does not turn over at $\gtrsim -12.5$. Usually at higher redshift the turn over magnitude is larger. Therefore it can be reasonably inferred that at $z > 6$ the LF will not turn over at least down to -12.5 . In this case the galaxies that ionized the Universe have already been uncovered (Robertson et al. 2013, 2015). However, their result was questioned by B17 who argued that L17 may overestimate the volume density at the faint end due to: 1) an excess of sources near the completeness limit; and 2) the assumption of too large intrinsic half-light radii. B17 investigated the impact of magnification errors on the LF carefully and found that at $M_{UV} \gtrsim -14$ the magnification errors are extremely high. They developed a new model that incorporates the magnification errors into the LF, and by analyzing four FFs clusters: A2744, M0416 plus MACSJ0717.5+3745 (M0717) and MACSJ1149.5+2223 (M1149) they obtained the constraints that the LF should not turn over at least at $M_{UV} < -15.3$ to -14.2 (1σ C.L.), consistent with C16a.

In this paper, we expand the analysis presented in C16a by adding new FFs data and improved lensing models to obtain number counts in the two additional FFs clusters and update the previous two clusters. Throughout this paper we use the following cosmological parameters: $\Omega_m = 0.308, \Omega_\Lambda = 0.692, \Omega_b = 0.048, h = 0.678, \sigma_8 = 0.815, n_s = 0.97$ (Planck Collaboration et al. 2016a), magnitudes are presented in AB system.

2. METHODS

2.1. Observations

The photometric catalogues of high- z galaxies used in the present paper are provided by the ASTRODEEP team (Castellano et al. 2016c; Merlin et al. 2016b; Di Criscienzo et al. 2017), and all the lensing models are provided by the FFs team on the project website³.

The high- z sample comprises all sources at $5.0 < z < 10.0$ (galaxies with redshift above 10 have less contribution to constraining the reionization feedback effects, see Y16.) and with intrinsic magnitude fainter than $H_{160}=29.5$ from the ASTRODEEP catalogs of FFs clusters A2744, M0416 (Merlin et al. 2016b; Castellano et al. 2016a), M0717 and M1149 (Di Criscienzo et al. 2017)⁴.

All catalogues include photometry from the available *HST* ACS and WFC3 bands (B435, V606, I814, Y105, J125, JH140, H160, see e.g. Lotz et al. 2017) and from deep K-band (Brammer et al. 2016) and IRAC 3.6 μm and 4.5 μm data (PI Capak). Sources are detected on the H160 band af-

ter removing foreground light both from bright cluster galaxies and the diffuse intra-cluster light (ICL) as described in detail in Merlin et al. (2016b). Foreground light is also removed from the *HST* bands before estimating photometry with SExtractor (Bertin & Arnouts 1996) in dual-image mode. Photometry from the lower resolution Ks and IRAC images has been obtained with T-PHOT v2.0 (Merlin et al. 2015, 2016a). Photometric redshifts for all the sources have been measured with six different techniques based on different codes and assumptions. The FFs sources are then assigned the median of the six available photometric redshift estimates in order to minimize systematics and improve the accuracy. The final typical error on the photo- z is $\sim 0.04 \times (1+z)$ (Castellano et al. 2016a; Di Criscienzo et al. 2017). The magnification for each observed source is estimated on the basis of the relevant photometric redshift from shear and mass surface density values at its barycenter of the light distribution. All models made available on the STSCI website⁵ are used.

Compared to C16a we update in this paper the A2744 and M0416 high- z samples by exploiting the improved v3 lensing models now available, and we include in the analysis number counts from other two additional clusters, M0717 and M1149. In Tab. 1 we list the clusters and the corresponding lensing models used in this paper. In Fig. 1 we show the number counts (galaxy number per magnitude bin) of the galaxies with $5 < z < 10$ in the fields of four FFs clusters (we do not use the data of the parallel blank fields), as a function of $H_{160,\text{int}}$, where $H_{160,\text{int}}$ is the demagnified apparent magnitude at the *HST* F160W band. For each cluster we reconstruct the galaxy number counts by using each lensing model listed in Tab. 1, then make the median of the counts.

2.2. An empirical description of the LF turn-over

Is there evidence of a “turn-over” in the faint-end of the high- z galaxy LFs from the available FFs data? To investigate this problem we adopt the following reference LF model – a standard Schechter formula modulated by a term that rapidly drops when the absolute UV magnitude M_{UV} is much larger than the turn-over magnitude M_{UV}^T , and rapidly approaches unity when $M_{UV} \ll M_{UV}^T$:

$$\Phi(M_{UV}, z) = 0.4 \ln(10) \Phi^* \exp[10^{-0.4(M_{UV} - M_{UV}^*)}] \times 10^{-0.4(1+\alpha)(M_{UV} - M_{UV}^*)} 0.5[(1 - \text{erf}(M_{UV} - M_{UV}^T))], \quad (1)$$

where erf is the error function. At the M_{UV}^T the LF drops to half the value of a standard Schechter LF. In addition to the three redshift-dependent Schechter parameters Φ^*, M_{UV}^* ,

³ <https://archive.stsci.edu/prepds/frontier/lensmodels/>

⁴ Download: <http://www.astrodeep.eu/frontier-fields-download/>;

Catalogue interface: <http://astrodeep.u-strasbg.fr/ff/index.html>

⁵ <http://www.stsci.edu/hst/campaigns/frontier-fields/Lensing-Models>

Table 1. The FFs clusters and lensing models used in this paper.

Cluster	Lensing model
Abell 2744 (A2744)	GLAFIC v3; Sharon v3; Williams v3; Zitrin-LTM-Gauss v3, Zitrin-NFW v3; CATS v3.1
MACSJ0416.1-2403 (M0416)	GLAFIC v3; Sharon v3; Williams v3.1; Zitrin-LTM-Gauss v3; Zitrin-LTM v3; CATS v3.1; Bradač v3; Diego v3
MACSJ0717.5+3745 (M0717)	GLAFIC v3; Sharon v2; Williams v1; Zitrin-LTM-Gauss v1; Zitrin-LTM v1; CATS v1; Bradač v1; Merten v1
MACSJ1149.5+2223 (M1149)	GLAFIC v3; Sharon v2.1; Williams v1; Zitrin-LTM-Gauss v1; Zitrin-LTM v1; CATS v1; Bradač v1; Merten v1

Relevant references for lensing models listed in the table: GLAFIC: [Kawamata et al. \(2016\)](#); [Ishigaki et al. \(2015\)](#); [Oguri \(2010\)](#). Sharon: [Johnson et al. \(2014\)](#); [Jullo et al. \(2007\)](#). Williams: [Priewe et al. \(2017\)](#); [Sebesta et al. \(2016\)](#); [Grillo et al. \(2015\)](#); [Mohammed et al. \(2014\)](#); [Liesenborgs et al. \(2006\)](#). Zitrin: [Zitrin et al. \(2013, 2009\)](#). CATS: [Jauzac et al. \(2015, 2014\)](#); [Richard et al. \(2014\)](#); [Jauzac et al. \(2012\)](#); [Jullo & Kneib \(2009\)](#). Bradač: [Hoag et al. \(2016\)](#); [Bradač et al. \(2009, 2005\)](#). Diego: [Diego et al. \(2015, 2007, 2005b,a\)](#). Merten: [Merten et al. \(2011, 2009\)](#). All models are available on the STSCI website.

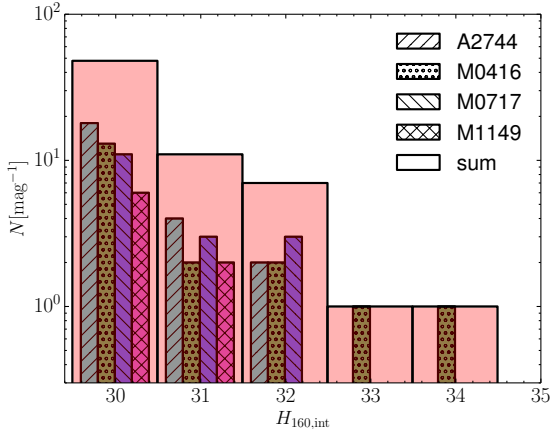


Figure 1. The galaxy number counts between $z = 5.0 - 10.0$ vs. demagnified H band apparent magnitude for the four FFs clusters. For each cluster we plot the median of the number counts reconstructed using lensing models listed in Tab. 1. We also plot the sum of the four clusters. Histograms in same group are in the same magnitude bin, for displaying purpose we shift their x-coordinates.

α , we introduce here a new one parameter M_{UV}^T . The M_{UV}^* is mainly determined by observations of bright galaxies and by large volume galaxy surveys while it is unconstrained in our lensed samples of ultra-faint galaxies. For this reason, and to focus on the LF turn-over relevant parameters only, we directly adopt the parameterization of M_{UV}^* from Sec. 5.1 of [Bouwens et al. \(2015b\)](#):

$$M_{UV}^* = -20.95 + 0.01 \times (z - 6), \quad (2)$$

discarding its uncertainties. We keep the Φ_* and α as free parameters that will be constrained together with M_{UV}^T from the FFs data.

2.3. A physically-motivated model of the high- z galaxy LFs

In Y16 we have developed a physically-motivated analytical model that describes the faint-end of the high- z galaxy LFs during the EoR. The model calibrates the “star formation efficiency” (defined as the star formation rate to halo dark

matter mass ratio) - halo mass relation using the Schechter formula of observed LF at redshift ~ 5 , then computes the luminosity of a halo according to its mass and formation time at any redshifts ([Mason et al. 2015](#), see also [Trenti et al. 2010](#) and [Tacchella et al. 2013](#)). Considering the probability distribution of a halo’s formation time ([Giocoli et al. 2007](#)), and the possibility of its star formation being quenched (if the circular velocity of this halo is smaller than a pre-assumed circular velocity criterion v_c^* and it is located in ionized regions), the LF is then derived from halo mass function. In this model, the LF does not necessarily decrease monotonically at its faint end but have complex shapes, see Fig. 6 and Fig. 7 in Y16.

The Y16 model has two free parameters, the escape fraction of ionizing photons, f_{esc} , and the critical circular velocity, v_c^* . The galaxy number counts are sensitive to v_c^* but less sensitive to f_{esc} , therefore we combine the number counts with the measured Thomson scattering optical depth to CMB photons, τ , to obtain the joint constraints.

2.4. Statistical framework

Here we summarise the procedure adopted to derive constraints on theoretical parameters from the observed galaxy number counts. A more detailed discussion can be found in C16a. Suppose in one cluster field we have observed N_{obs}^i galaxies in the i th of n_b magnitude bins, and by Monte Carlo simulation we compute (we include in the analysis the completeness as a function image size, and the intrinsic galaxy size - luminosity relation is from [Huang et al. \(2013\)](#), which is comparable with the relation used in [Bouwens et al. \(2017a,b\)](#), see C16a. See also [Kawamata et al. 2017](#) who however find steeper relation slope for galaxies down to $M_{UV} \sim -12.3$ in FFs) the probability to observe such number of galaxies, $p_1(N_{obs}^i | \mathbf{a})$ (see Eq. 3 of C16a), in a model with parameter set \mathbf{a} (suppose \mathbf{a} has n_a elements), then we can build the likelihood:

$$L \propto \left[\prod_i^{n_b} p_1(N_{obs}^i | \mathbf{a}) \right] \times p_2(\mathbf{a}), \quad (3)$$

where p_2 is an additional constraint either from other independent observations, or from given priors. For example, if priors $\mathbf{b} = (b_1, b_2, \dots)$ with variance $\sigma_{\mathbf{b}} = (\sigma_{b_1}, \sigma_{b_2}, \dots)$ are considered,

$$p_2(\mathbf{a}) \propto \prod_i^{n_a} \exp\left(-\frac{(a_i - b_i)^2}{2\sigma_{b_i}^2}\right). \quad (4)$$

Or if we consider the CMB scattering optical depth as another independent observation,

$$p_2(\mathbf{a}) \propto \exp\left(-\frac{[\tau(\mathbf{a}) - \tau_{\text{obs}}]^2}{2\sigma_{\tau}^2}\right). \quad (5)$$

The constraints on \mathbf{a} are obtained by looking for the minimum of $\chi^2 = -2\log(L)$, χ_{min}^2 , and the contours corresponding to $\chi_{\text{min}}^2 + \Delta\chi^2$.

3. RESULTS

3.1. Is a LF turn-over observed at $z \sim 6$?

In this subsection we investigate the constraints on parameters in the empirical model in Sec. 2.2 at $z \sim 6$ by analyzing galaxy samples with $5 < z < 7$ in ASTRODEEP catalog. We vary Φ_* in the range $\Phi_* \leq 1.5 \times 10^{-3} \text{ Mpc}^{-3}$, α in the range $-2.5 \leq \alpha \leq -1.6$ and M_{UV}^T in the range $-10 \geq M_{\text{UV}}^T \geq -18$.

Using a collection of wide and deep blank field survey data Bouwens et al. (2015b) (B15) have obtained constraints on both Φ_* and α , we use these constraints as priors (see Eq. 3) in the empirical model, namely:

$$p_2(\Phi_*, \alpha) = \exp\left[-\frac{(\Phi_* - \Phi_*^{\text{B15}})^2}{2\sigma_{\Phi_*^{\text{B15}}}^2}\right] \times \exp\left[-\frac{(\alpha - \alpha^{\text{B15}})^2}{2\sigma_{\alpha^{\text{B15}}}^2}\right]. \quad (6)$$

Explicitly, we use $\Phi_*^{\text{B15}} = 0.5 \times 10^{-3} \text{ Mpc}^{-3}$ and $\sigma_{\Phi_*^{\text{B15}}} = 0.22 \times 10^{-3} \text{ Mpc}^{-3}$, $\alpha^{\text{B15}} = -1.87$ and $\sigma_{\alpha^{\text{B15}}} = 0.1$, which are B15 constraints at $z \sim 6$. This is a simple way to fairly take into account the contribution from blank field surveys with large volume, thereby reducing the uncertainties. We obtain the combined constraint from different lensing models by using their mean probability as p_1 in Eq. 3, as discussed in C16a (see their Eq. 3).

The results of this analysis are shown in Fig. 2. In the 2D M_{UV}^T - α contour map the Φ_* has been marginalized, and in the M_{UV}^T - Φ_* contour map the α has been marginalized. We can see that at 2σ C.L., the upper boundary of M_{UV}^T is always open. To obtain the final constraints we marginalize both Φ_* and α , and we have $M_{\text{UV}}^T \gtrsim -14.3$ at 2σ C.L.. Still, we only find the lower boundary of M_{UV}^T , the upper boundary is open. This implies that no evidence is found in the existing data for the four FFs clusters of a LF turn-over at $z \approx 6$. We summarise the constraints in Tab. 2.

We plot the LF corresponding to the M_{UV}^T constraints at $z \sim 6$ in bottom right panel of Fig. 2. As a reference and

consistency check, we also plot the B15 LF data, and the LF data constructed from A2744, M0416 and M0717 and their corresponding parallel blank field in A15 at $z \sim 7$, which is one of the deepest LFs and consistent with other LFs in the overlap magnitude range. We do not show our observational data because we do not try to reconstruct LF from the number counts. It is seen in the bottom panel that our fit is consistent with the behavior of A15 data at the faint-end.

We now investigate the systematic differences between the various lensing models. In Fig. 3 we show the α - M_{UV}^T constraints by using only one lensing model each time, ignoring version discrepancies. Each of ‘‘GLAFIC’’, ‘‘CATS’’, ‘‘Sharon’’, ‘‘Williams’’ and ‘‘Zitrin-LTM-Gauss’’ is shown by one column in Fig. 3. We choose these five lensing models because they are available for all the four clusters; and at least for A2744 and M0416 the versions are equal or later than v3.0. For each lensing model from top to bottom the panels are α - M_{UV}^T constraints, the sum of the number counts for the four FFs clusters and the LFs corresponding to the constraints on M_{UV}^T (see Tab. 2).

Indeed, the discrepancies between lensing models are rather evident, especially for the M_{UV}^T upper boundaries. This is because although the number counts (the middle panels of Fig. 3) are basically consistent with each at $H_{160,\text{int}} \lesssim 32$, at the faintest end they are rather different from each other. Particularly, for the GLAFIC model there is marginal evidence (at 1σ C.L.) for the existence of M_{UV}^T upper limit, ~ -13.6 , implying that the number of observed faint galaxies might be slightly lower than the extrapolation of a Schechter LF. However, given the low significance, we refrain from speculating further on it. Clearly, to robustly confirm such a turn-over at $\gtrsim 2\sigma$ C.L. more data is needed. In all the cases, above 2σ C.L. the upper boundaries are open, implying that no turn-over is apparent.

3.2. Constraints on v_c^*

We then investigate the constraints we can put on the physically-motivated model. Since in this model both f_{esc} and v_c^* are redshift independent parameters, we use all the data in $z = 5.0 - 10.0$. In top panel of Fig. 4 we show the constraints on f_{esc} and v_c^* , using the combination of galaxy number counts in the FFs fields and the latest *Planck*2016 Thomson scattering optical depth to CMB photons: $\tau = 0.058 \pm 0.012$ (Planck Collaboration et al. 2016b). Compared with C16a, the smaller τ helps us to obtain tighter constraints on f_{esc} , say $f_{\text{esc}} \lesssim 63\%$ (2σ C.L.) after marginalizing v_c^* . If marginalize f_{esc} we find $v_c^* \lesssim 57 \text{ km s}^{-1}$ (2σ C.L.), which corresponds to a halo mass $M = 3.3 \times 10^9 M_{\odot}$ ($8.3 \times 10^9 M_{\odot}$) and absolute UV magnitude $M_{\text{UV}} \approx -14.5$ (-14.9), at $z = 10$ (5), i.e. slightly tighter than C16a (see Fig. 3 there). Additional constraints are listed in Tab. 2, where we present both 1σ and 2σ constraints. The LFs at $z \sim 6$ and 8

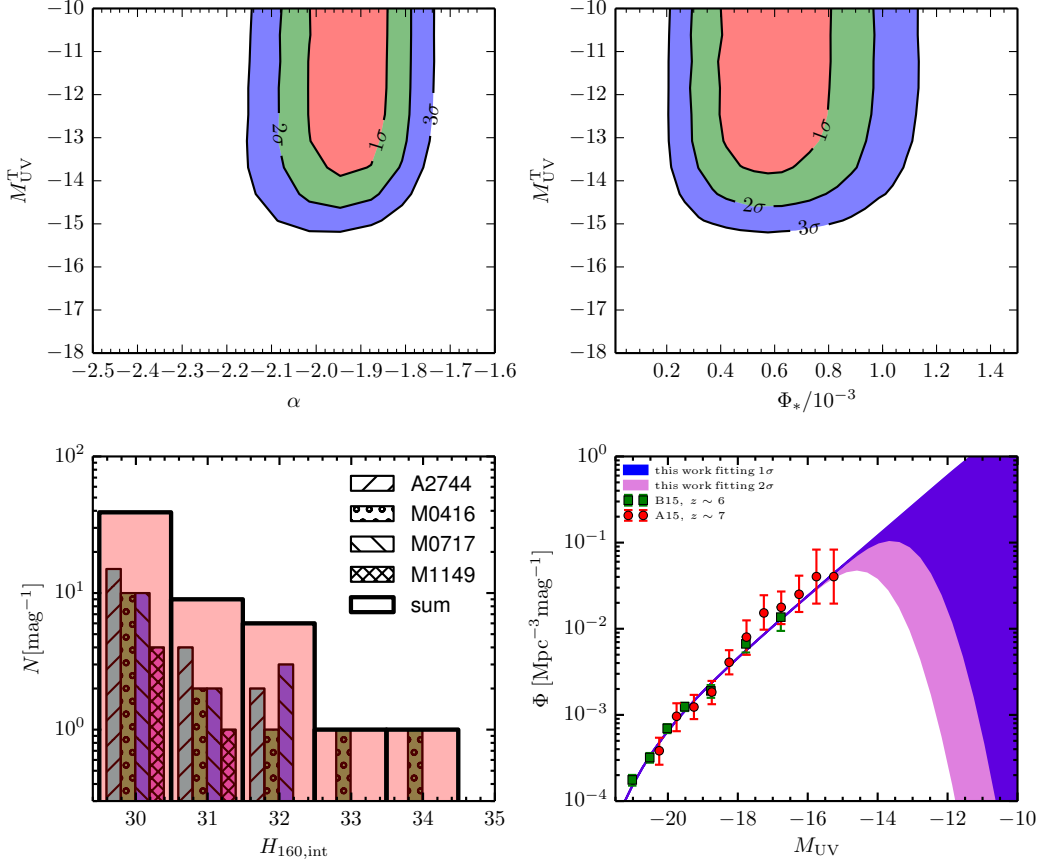


Figure 2. The constraints on α , Φ_* and M_{UV}^T from the combination of all the four FFs clusters. The two top panels are the α - M_{UV}^T and Φ_* - M_{UV}^T contour maps respectively. In each case the remaining parameter has been marginalized. The bottom left panel is the observed number count of galaxies with $z \sim 5-7$ for the FFs clusters. The bottom right panel is the LF fit of present work at $z \sim 6$, together with the B15 LF data and the A15 LF data.

Table 2. Constraints on M_{UV}^T and v_c^*

	ALL	GLAFIC	CATS	Sharon	Williams	Zitrin-LTM-Gauss
1 σ C.L.	$M_{UV}^T \gtrsim -13.3$	$-13.6 \gtrsim M_{UV}^T \gtrsim -15.3$	$M_{UV}^T \gtrsim -11.4$	$M_{UV}^T \gtrsim -13.6$	$M_{UV}^T \gtrsim -13.5$	$M_{UV}^T \gtrsim -11.9$
2 σ C.L.	$M_{UV}^T \gtrsim -14.3$	$M_{UV}^T \gtrsim -15.8$	$M_{UV}^T \gtrsim -12.5$	$M_{UV}^T \gtrsim -14.7$	$M_{UV}^T \gtrsim -14.7$	$M_{UV}^T \gtrsim -13.2$
1 σ C.L.	$v_c^* \lesssim 47$ km s $^{-1}$	$v_c^* \lesssim 40$ km s $^{-1}$	$v_c^* \lesssim 32$ km s $^{-1}$	$v_c^* \lesssim 51$ km s $^{-1}$	$v_c^* \lesssim 49$ km s $^{-1}$	$v_c^* \lesssim 39$ km s $^{-1}$
2 σ C.L.	$v_c^* \lesssim 57$ km s $^{-1}$	$v_c^* \lesssim 60$ km s $^{-1}$	$v_c^* \lesssim 52$ km s $^{-1}$	$v_c^* \lesssim 66$ km s $^{-1}$	$v_c^* \lesssim 60$ km s $^{-1}$	$v_c^* \lesssim 50$ km s $^{-1}$

in Y16 model corresponding to no feedback, $v_c^* = 47$ and 57 km s $^{-1}$ for $f_{esc} = 0.15$ are shown in bottom panels of Fig. 4.

We also find that different clusters do not contribute equally to the final constraint. If we respectively *remove* one of A2744, M0416, M0717 and M1149 each time, we obtain $v_c^* \lesssim 58, 70, 57$ and 56 km s $^{-1}$ (all at 2σ C.L.) respectively. As seen in Fig. 1, this is because the M0416 field is deeper than the others, thus having a larger influence in the final constraint.

We also investigate the discrepancies between different lensing models in this case. When using one lensing model

at a time, as mentioned in the last subsection, we obtain the 2σ C.L. constraints: $v_c^* \lesssim 60$ (GLAFIC), 52 (CATS), 66 (Sharon), 60 (Williams) and 50 (Zitrin-LTM-Gauss) km s $^{-1}$ respectively, see Tab. 2.

4. CONCLUSIONS

We investigated the LF of galaxies in the reionization epoch at low luminosities under the explicit assumption that any deviation from a pure Schechter LF at faint magnitudes is imprinted by feedback effects during reionization itself. We considered two LF models, and obtained con-

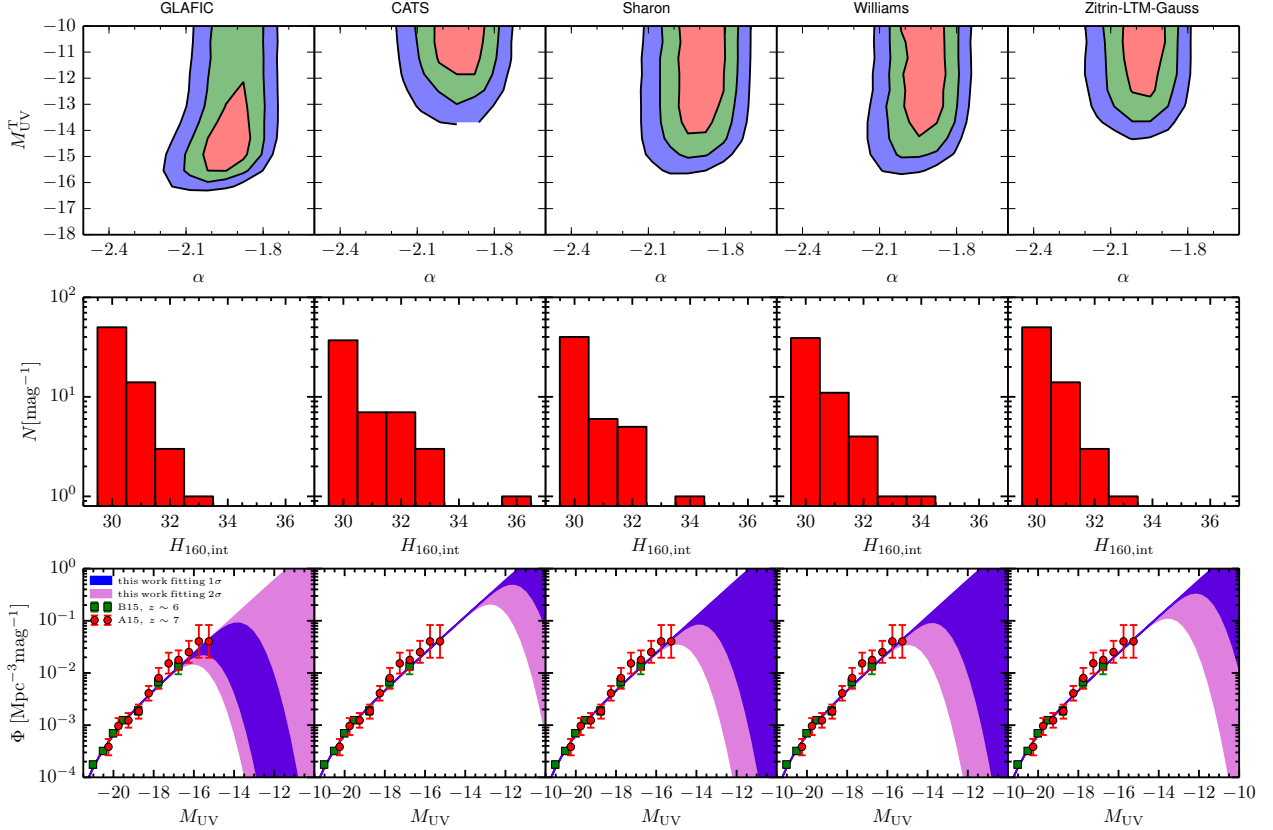


Figure 3. *Top panels:* The constraints on parameters α and M_{UV}^T from five individual lensing models (marked in the panel), “GLAFIC”, “CATS”, “Sharon”, “Williams” and “Zitrin-LTM-Gauss” from the four FFs clusters data in $z \sim 5-7$. *Middle panels:* The sum of the number counts for the four FFs clusters in $z \sim 5-7$ for the five lensing models. *Bottom panels:* The LFs corresponding to the 1σ C.L. and 2σ C.L. constraints on M_{UV}^T .

straints on their parameters from the observed high- z ultrafaint galaxy number counts in four FFs gravitational lensing cluster fields. We first test an empirical model where the standard Schechter formula is modulated by the suppressing term $0.5[1 - \text{erf}(M_{UV} - M_{UV}^T)]$. The LF is unchanged when $M_{UV} \ll M_{UV}^T$, and drops rapidly when $M_{UV} \gg M_{UV}^T$. Secondly, we consider the physically-motivated model proposed by Y16 and analysed in C16a. In this model the star formation is quenched in halos with circular velocity smaller than v_c^* , during and after the EoR, as long as they are located in ionized regions. As a result, the LF has complex behavior at low luminosities.

We used the photometric catalogs and redshifts of the four FF clusters A2744, M0416, M0717 and M1149 provided by the ASTRODEEP collaboration. The first two clusters have already been analyzed in a previous work C16a, therefore in this paper we only considered the lensing models with versions later than 3.0, which were not adopted in C16a. For other two clusters, we used all available lensing models, and where multiple versions are available we adopted the latest ones.

For the empirical model, at 1σ (2σ) C.L. we have obtained constraints $M_{UV}^T \gtrsim -13.3$ ($M_{UV}^T \gtrsim -14.3$) at $z \sim 6$. We therefore concluded that we have not yet confirmed the LF turn-over in the data of these four FFs clusters.

We clarify a dissimilarity between the definition of the “turn-over magnitude” between B17 and our work. In B17, the turn-over magnitude is the absolute magnitude at which the LF’s derivative is zero, while in our work it is defined as the absolute magnitude where the LF decreases to half of the Schechter LF. Moreover, their LF-end is modulated by a term $10^{-0.4\delta(M_{UV}+16)^2}$ which could decrease gently even when M_{UV} is higher than the turn-over magnitude, depending on δ . However we assume the modulation term $0.5[1 - \text{erf}(M_{UV} - M_{UV}^T)]$, at $M_{UV} > M_{UV}^T$ the LF drops rapidly. For the above reason, we do not directly compare our M_{UV}^T with B17. Instead, we plot our constrained LF together with the LF constructed in B17, see Fig. 5. From this figure, the B17 LF constraint could be approximately translated into $M_{UV}^T \gtrsim -14$ of our model, a bit shallower than what we found in our work, $M_{UV}^T \gtrsim -13.3$. This difference might be due to the different methodologies adopted to take into account sys-

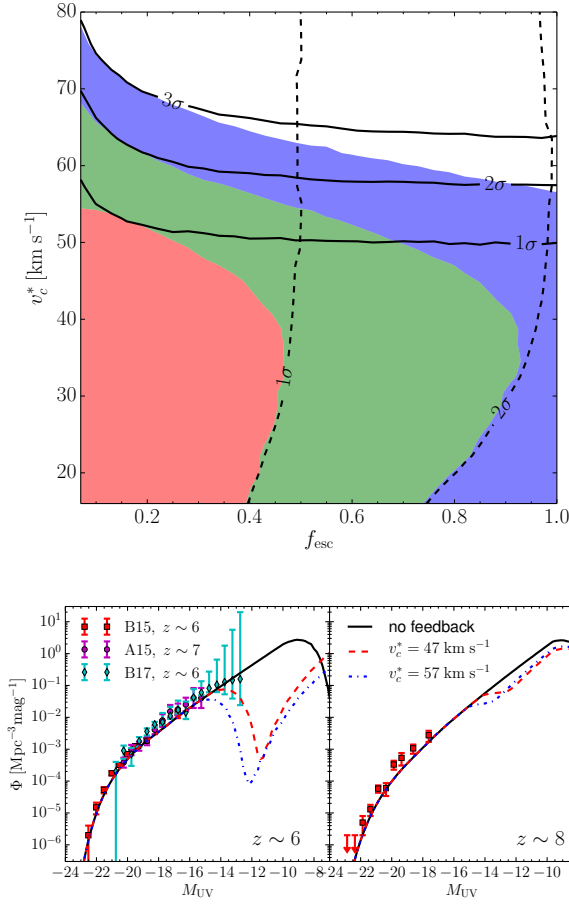


Figure 4. *Top:* The contour map of constraints on f_{esc} and v_c^* obtained by using the combination of galaxy number counts in four FFs clusters and the *Planck*2016 CMB scattering optical depth $\tau = 0.058 \pm 0.012$ (Planck Collaboration et al. 2016b). Solid curves mean the constraints obtained from galaxy number counts only, dashed lines mean from the CMB only, filled regions mean constraints from their combination. *Bottom:* The LFs at $z \sim 6$ and 8 corresponding to no feedback, $v_c^* = 47$ and 57 km s $^{-1}$, we set $f_{\text{esc}} = 0.15$.

tematic effects. We use the median of the number counts from difference lensing models as the true number count, while B17 incorporates systematics estimated by the difference between the various models. As a conservative check, in our work if we drop the galaxies with magnification > 100 in observations and we obtain constraints $M_{\text{UV}}^{\text{T}} \gtrsim -14.8$ (-15.5) at 1σ (2σ) C.L..

One difference between our work and L17 is that, in our case, we first construct the number count for each lensing model independently, then take the median of the number counts from different lensing models; it excludes the number count in extremely faint magnitude bins where only in a few lensing models there are galaxies detected; while in L17, for the image of each galaxy they take the flux-weighted magnification of different lensing models, then construct the LF.

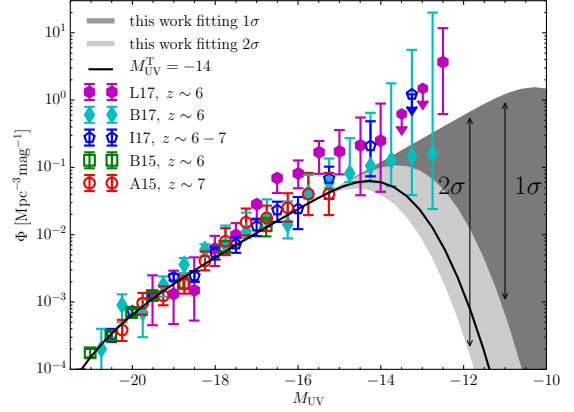


Figure 5. The B15, A15, B17, L17 and I17 observations, the LF corresponding to 1σ C.L. constraints $M_{\text{UV}}^{\text{T}} \gtrsim -13.3$ and 2σ C.L. constraints $M_{\text{UV}}^{\text{T}} \gtrsim -14.3$, and a LF with $M_{\text{UV}}^{\text{T}} = -14$.

Another difference is, we have used the $\alpha = -1.87 \pm 0.10$ as the priors of the LF slope, while in the L17 the data favors a steeper slope ~ -2.1 . We also plot the L17 and I17 data in Fig. 5, together with our LF fittings.

For the physically-motivated model we obtained $v_c^* \lesssim 57$ km s $^{-1}$ at 2σ C.L., corresponding to absolute UV magnitude -14.5 at $z = 10$ and -14.9 at $z = 5$. Considering the discrepancies between different lensing models, we have $v_c^* \lesssim 52-66$ km s $^{-1}$. In all the cases considered, we have not found the lower limit for v_c^* .

Thanks to the combined power of gravitational lensing and deep *HST* multi-band imaging we are just starting to observe the faintest galaxy populations likely responsible for reionization. The present analysis and similar ones in the past have not yet found significant evidence of the presence of feedback effects suppressing the formation of galaxies at faint UV magnitudes. This is likely due to the uncertainties and systematics involved in lensing models and in the selection and characterization of distant, faint sources. In this respect, the completion of the FFs survey, and improvements in lensing model accuracy as well as high redshift sample selection enabled by future *JWST* photometric and spectroscopic observations will be crucial for improving our understanding of reionization.

This work utilizes gravitational lensing models produced by PIs Bradač, Natarajan & Kneib (CATS), Merten & Zitrin, Sharon, and Williams, and the GLAFIC and Diego groups. This lens modeling was partially funded by the HST Frontier Fields program conducted by STScI. STScI is operated by the Association of Universities for Research in Astronomy, Inc. under NASA contract NAS 5-26555. The lens models were obtained from the Mikulski Archive for Space Telescopes (MAST). BY is supported by the CAS Pi-

oneer Hundred Talents (Young Talents) Program. RA acknowledges support from the ERC Advanced Grant 695671 ÒQUENCHÓ. M.J.M. acknowledges the support of the National Science Centre, Poland through the POLONEZ grant

2015/19/P/ST9/04010. This project has received funding from the European Union's Horizon 2020 research and innovation programme under the Marie Skłodowska-Curie grant agreement No. 665778.

REFERENCES

- Atek, H., Richard, J., Jauzac, M., et al. 2015a, *ApJ*, **814**, 69, [A15]
- Atek, H., Richard, J., Kneib, J.-P., et al. 2015b, *ApJ*, **800**, 18
- Bertin, E., & Arnouts, S. 1996, *A&AS*, **117**, 393
- Bouwens, R. J., Illingworth, G. D., Oesch, P. A., et al. 2017a, *ApJ*, **843**, 41
- . 2015a, *ApJ*, **811**, 140
- Bouwens, R. J., Oesch, P. A., Illingworth, G. D., Ellis, R. S., & Stefanon, M. 2017b, *ApJ*, **843**, 129, [B17]
- Bouwens, R. J., Illingworth, G. D., Oesch, P. A., et al. 2015b, *ApJ*, **803**, 34, [B15]
- Bradač, M., Schneider, P., Lombardi, M., & Erben, T. 2005, *A&A*, **437**, 39
- Bradač, M., Treu, T., Applegate, D., et al. 2009, *ApJ*, **706**, 1201
- Brammer, G. B., Marchesini, D., Labbé, I., et al. 2016, *ApJS*, **226**, 6
- Castellano, M., Yue, B., Ferrara, A., et al. 2016a, *ApJL*, **823**, L40, [C16a]
- Castellano, M., Dayal, P., Pentericci, L., et al. 2016b, *ApJL*, **818**, L3
- Castellano, M., Amorín, R., Merlin, E., et al. 2016c, *A&A*, **590**, A31
- Ceverino, D., Glover, S. C. O., & Klessen, R. S. 2017, *MNRAS*, **470**, 2791
- Choudhury, T. R., & Ferrara, A. 2007, *MNRAS*, **380**, L6
- Choudhury, T. R., Ferrara, A., & Gallerani, S. 2008, *MNRAS*, **385**, L58
- Dayal, P., Dunlop, J. S., Maio, U., & Ciardi, B. 2013, *MNRAS*, **434**, 1486
- Dayal, P., Mesinger, A., & Pacucci, F. 2015, *ApJ*, **806**, 67
- Di Criscienzo, M., Merlin, E., Castellano, M., et al. 2017, ArXiv e-prints, [arXiv:1706.03790](https://arxiv.org/abs/1706.03790)
- Diego, J. M., Protopapas, P., Sandvik, H. B., & Tegmark, M. 2005a, *MNRAS*, **360**, 477
- Diego, J. M., Sandvik, H. B., Protopapas, P., et al. 2005b, *MNRAS*, **362**, 1247
- Diego, J. M., Tegmark, M., Protopapas, P., & Sandvik, H. B. 2007, *MNRAS*, **375**, 958
- Diego, J. M., Broadhurst, T., Benitez, N., et al. 2015, *MNRAS*, **446**, 683
- Finlator, K., Prescott, M. K. M., Oppenheimer, B. D., et al. 2017, *MNRAS*, **464**, 1633
- Giallongo, E., Grazian, A., Fiore, F., et al. 2015, *A&A*, **578**, A83
- Giocoli, C., Moreno, J., Sheth, R. K., & Tormen, G. 2007, *MNRAS*, **376**, 977
- Gnedin, N. Y. 2016, *ApJL*, **825**, L17
- González-López, J., Bauer, F. E., Romero-Cañizales, C., et al. 2017a, *A&A*, **597**, A41
- González-López, J., Bauer, F. E., Aravena, M., et al. 2017b, ArXiv e-prints, [arXiv:1704.03007](https://arxiv.org/abs/1704.03007)
- Grillo, C., Suyu, S. H., Rosati, P., et al. 2015, *ApJ*, **800**, 38
- Hoag, A., Huang, K.-H., Treu, T., et al. 2016, *ApJ*, **831**, 182
- Huang, K.-H., Ferguson, H. C., Ravindranath, S., & Su, J. 2013, *ApJ*, **765**, 68
- Ishigaki, M., Kawamata, R., Ouchi, M., Oguri, M., & Shimasaku, K. 2017, ArXiv e-prints, [arXiv:1702.04867](https://arxiv.org/abs/1702.04867), [I17]
- Ishigaki, M., Kawamata, R., Ouchi, M., et al. 2015, *ApJ*, **799**, 12
- Jauzac, M., Jullo, E., Kneib, J.-P., et al. 2012, *MNRAS*, **426**, 3369
- Jauzac, M., Clément, B., Limousin, M., et al. 2014, *MNRAS*, **443**, 1549
- Jauzac, M., Richard, J., Jullo, E., et al. 2015, *MNRAS*, **452**, 1437
- Johnson, T. L., Sharon, K., Bayliss, M. B., et al. 2014, *ApJ*, **797**, 48
- Jullo, E., & Kneib, J.-P. 2009, *MNRAS*, **395**, 1319
- Jullo, E., Kneib, J.-P., Limousin, M., et al. 2007, *New Journal of Physics*, **9**, 447
- Kawamata, R., Ishigaki, M., Shimasaku, K., et al. 2017, ArXiv e-prints, [arXiv:1710.07301](https://arxiv.org/abs/1710.07301)
- Kawamata, R., Oguri, M., Ishigaki, M., Shimasaku, K., & Ouchi, M. 2016, *ApJ*, **819**, 114
- Laporte, N., Infante, L., Troncoso Iribarren, P., et al. 2016, *ApJ*, **820**, 98
- Liesenborgs, J., De Rijcke, S., & Dejonghe, H. 2006, *MNRAS*, **367**, 1209
- Liu, C., Mutch, S. J., Angel, P. W., et al. 2016, *MNRAS*, **462**, 235
- Livermore, R. C., Finkelstein, S. L., & Lotz, J. M. 2017, *ApJ*, **835**, 113, [L17]
- Lotz, J. M., Koekemoer, A., Coe, D., et al. 2017, *ApJ*, **837**, 97
- Madau, P., & Haardt, F. 2015, *ApJL*, **813**, L8
- Mashian, N., Oesch, P. A., & Loeb, A. 2016, *MNRAS*, **455**, 2101
- Mason, C. A., Trenti, M., & Treu, T. 2015, *ApJ*, **813**, 21
- McLure, R. J., Dunlop, J. S., Bowler, R. A. A., et al. 2013, *MNRAS*, **432**, 2696
- Menci, N., Merle, A., Totzauer, M., et al. 2017, *ApJ*, **836**, 61
- Menci, N., Sanchez, N. G., Castellano, M., & Grazian, A. 2016, *ApJ*, **818**, 90

- Merlin, E., Fontana, A., Ferguson, H. C., et al. 2015, *A&A*, **582**, [A15](#)
- Merlin, E., Bourne, N., Castellano, M., et al. 2016a, *A&A*, **595**, [A97](#)
- Merlin, E., Amorín, R., Castellano, M., et al. 2016b, *A&A*, **590**, [A30](#)
- Merten, J., Cacciato, M., Meneghetti, M., Mignone, C., & Bartelmann, M. 2009, *A&A*, **500**, [681](#)
- Merten, J., Coe, D., Dupke, R., et al. 2011, *MNRAS*, **417**, [333](#)
- Mitra, S., Choudhury, T. R., & Ferrara, A. 2016, ArXiv e-prints, [arXiv:1606.02719](#)
- Mohammed, I., Liesenborgs, J., Saha, P., & Williams, L. L. R. 2014, *MNRAS*, **439**, [2651](#)
- Ogorean, G. A., van Weeren, R. J., Jones, C., et al. 2015, *ApJ*, **812**, [153](#)
- . 2016, *ApJ*, **819**, [113](#)
- Oguri, M. 2010, *PASJ*, **62**, [1017](#)
- Planck Collaboration, Ade, P. A. R., Aghanim, N., et al. 2016a, *A&A*, **594**, [A13](#)
- Planck Collaboration, Adam, R., Aghanim, N., et al. 2016b, *A&A*, **596**, [A108](#)
- Priewe, J., Williams, L. L. R., Liesenborgs, J., Coe, D., & Rodney, S. A. 2017, *MNRAS*, **465**, [1030](#)
- Richard, J., Jauzac, M., Limousin, M., et al. 2014, *MNRAS*, **444**, [268](#)
- Robertson, B. E., Ellis, R. S., Furlanetto, S. R., & Dunlop, J. S. 2015, *ApJL*, **802**, [L19](#)
- Robertson, B. E., Furlanetto, S. R., Schneider, E., et al. 2013, *ApJ*, **768**, [71](#)
- Salvaterra, R., Ferrara, A., & Dayal, P. 2011, *MNRAS*, **414**, [847](#)
- Salvaterra, R., Maio, U., Ciardi, B., & Campisi, M. A. 2013, *MNRAS*, **429**, [2718](#)
- Sebesta, K., Williams, L. L. R., Mohammed, I., Saha, P., & Liesenborgs, J. 2016, *MNRAS*, **461**, [2126](#)
- Sun, G., & Furlanetto, S. R. 2016, *MNRAS*, **460**, [417](#)
- Tacchella, S., Trenti, M., & Carollo, C. M. 2013, *ApJL*, **768**, [L37](#)
- Trenti, M., Stiavelli, M., Bouwens, R. J., et al. 2010, *ApJL*, **714**, [L202](#)
- van Weeren, R. J., Ogorean, G. A., Jones, C., et al. 2017, *ApJ*, **835**, [197](#)
- Weisz, D. R., Johnson, B. D., & Conroy, C. 2014, *ApJL*, **794**, [L3](#)
- Xu, H., Wise, J. H., Norman, M. L., Ahn, K., & O’Shea, B. W. 2016, *ApJ*, **833**, [84](#)
- Yue, B., Ferrara, A., Vanzella, E., & Salvaterra, R. 2014, *MNRAS*, **443**, [L20](#)
- Yue, B., Ferrara, A., & Xu, Y. 2016, *MNRAS*, **463**, [1968](#), [Y16]
- Zitrin, A., Broadhurst, T., Umetsu, K., et al. 2009, *MNRAS*, **396**, [1985](#)
- Zitrin, A., Meneghetti, M., Umetsu, K., et al. 2013, *ApJL*, **762**, [L30](#)